JOURNAL OF CATALYSIS 123, 60–73 (1990)

Effect of Zeolite Protons on Palladium-Catalyzed Hydrocarbon Reactions

S. T. HOMEYER, Z. KARPIŃSKI,[1] AND W. M. H. SACHTLER[2]

V. N. Ipatieff Laboratory, Center of Catalysis and Surface Science, Department of Chemistry, Northwestern University, Evanston, Illinois 60608

Received September 22, 1989; revised December 4, 1989

Catalytic superactivity of electron-deficient palladium for neopentane conversion, previously reported for Pd/Al_2O_3, has been verified for Pd/NaHY. The reaction rate, per accessible Pd atom, correlates with the proton content of the catalysts; for samples that contain all the protons generated during H_2 reduction of Pd, it is two orders of magnitude higher than that for Pd/SiO_2. Samples prepared by reduction of $Pd(NH_3)_2^{2+}NaY$ display an intermediate activity. It is suggested that Pd-proton adducts are highly active sites in neopentane conversion. With methylcyclopentane as a catalytic probe, all Pd/NaHY samples deactivate rapidly and coke is deposited. Temperature-programmed oxidation reveals two types of coke, one of which correlates with the proton concentration in the catalyst.

I. INTRODUCTION

The catalytic signature of a zeolite-supported transition metal often differs significantly from that of the same metal on an amorphous support. Three basic causes that can be identified for these differences are: (1) metal particle morphology, (2) chemical interaction of the metal and support, and (3) the nature of the coproduct of metal reduction. On zeolites, the metal particles tend to be more uniform in size and shape due to geometric constraints of the zeolite lattice (*1–3*). In previous papers, we reported on the effects of the morphology of these encaged particles on catalyst selectivity and activity (*4–7*). Chemical interaction of metals and amorphous supports has been the subject of much research. Clearly, such chemical reactions are specific for the nature of the support and often absent for zeolite supports. The present paper is focused on the third aspect, i.e., effects of the coproduct of metal/zeolite reduction.

In the case of amorphous supports, impregnation of a metal precursor, followed by calcination, will result in the formation of a supported metal oxide or halide. Reduction in a hydrogen flow then leads to formation of metal particles and H_2O or hydrogen halide. In many instances of catalytic interest, the coproduct will be volatile and thus will not form a major constituent of the reduced catalyst. For zeolite supports, however, the metal precursor is often introduced by cation exchange; reduction of these cations with hydrogen leads to the formation of protons of high Brønsted acidity, e.g.,

$$Pd^{2+} + H_2 \rightarrow Pd^0 + 2H^+. \qquad (1)$$

These acid sites provide a bifunctional character to metal/zeolite catalysts (*8*). As the metal atoms will agglomerate to particles, but the protons remain isolated, the concentration of the zeolite protons will significantly exceed the concentration of surface-exposed transition metal atoms, even if the zeolite was nonacidic prior to the ion exchange with the metal precursor.

The above statement must be modified if calcination prior to reduction did not com-

[1] Institute of Physical Chemistry, Polish Academy of Sciences, Warsaw, Poland.

[2] To whom correspondence should be sent.

0021-9517/90 $3.00

pletely destroy the ligand shell of complexed transition metal ions. A case in point is Pd/NaY, prepared by ion exchange of $Pd(NH_3)_4^{2+}$ ions. In previous work, we investigated the elementary steps which occur during the genesis of Pd/NaY (*9–11*). It was shown that calcination destroys the ammine ligands in steps; consequently, calcination in O_2 at moderate temperatures ($T_C \leq 250°C$) leaves the ammine shell partially intact, resulting in the formation of $Pd(NH_3)_x^{2+}$. Quantitative analysis of the gases consumed and formed during temperature-programmed reduction and temperature-programmed oxidation showed that after calcination at 250°C, the majority of the palladium ions are present as a diammine complex, $Pd(NH_3)_2^{2+}$, located in supercages (*9–11*). During subsequent hydrogen reduction of these complexes inside the zeolite, the ammine ligands react with protons forming NH_4^+ ions:

$$Pd(NH_3)_2^{2+} + H_2 \rightarrow Pd^0 + 2NH_4^+. \quad (2)$$

Under these conditions, the resulting catalyst does not expose numerous strong acid sites, at least not in the initial state of its operation as a catalyst. Our previous work further shows that the NH_4^+ ions in NaY are remarkably stable; they are likely to survive conditions of hydrocarbon conversion catalysis at $T < 300°C$. It thus follows that the coproduct of hydrogen reduction of zeolite-supported transition metals may consist of protons of high Brønsted acidity, but their actual concentration will largely depend on the conditions of the preceding catalyst calcination.

The objective of the present paper is to investigate the effects of zeolite protons on the catalytic operation of zeolite-supported Pd catalyst. We, therefore, chose to examine the catalytic behavior of supported Pd of different proton concentrations. The distinguishing characteristics of three types of samples are as follows:

(1) $Pd(NH_3)_4/NaY$ ($T_C = 500°C$, $T_R = 350°C$, where T_C and T_R stand for the temperatures of calcination and reduction). These pretreatment conditions yield a high concentration of protons as coproduct of catalyst reduction. These catalysts will be referred to as Pd/NaY-500.

(2) $Pd(NH_3)_4/NaY$ ($T_C = 250°C$, $T_R = 300°C$). In these samples, ammonium ions are the major coproduct of catalyst reduction. These samples will further be referred to as Pd/NaY-250.

(3) Pd/SiO_2 ($T_C = 300°C$, $T_R = 300°C$). These catalysts were prepared by impregnation of $Pd(NO_3)_2$. Reduction of the PdO formed during calcination yields metal particles and water.

In type (1), all protons created during reduction are available for reaction. In type (2), however, most protons are trapped in ammonium ions. Their decomposition under reducing conditions is appreciably fast at temperatures near or above 350°C (*9*). When tested at lower temperatures, the acidic function of these catalysts should remain largely neutralized. It has also been reported that ammonia injections are effective in neutralizing acidity generated by reduction of Pt ions in Pt/ZSM-5 olefin hydrogenation catalysts (*12*). No protons are in catalysts of type (3). The Brønsted acidity of the three catalyst types should thus decrease in the order: (1) > (2) > (3).

In order to put the scope of this work into perspective, we shall first mention what effects of protons can be envisaged in hydrocarbon conversion reactions. In our opinion, it is useful to classify the anticipated effects of zeolithic protons on metal catalysis in four main categories:

1. Oxidation of Metal Atoms by Protons

In previous work with Pt/NaY (*13, 14*) and Pt/HY (*14*), we were able to show that isolated Pt atoms in sodalite cages of NaY are oxidized by protons in reversal of the metal reduction process:

$$2H^+ + Pt^0 \rightarrow Pt^{2+} + H_2. \quad (3)$$

For Ni/NaY, this reoxidation is not confined to isolated metal atoms (*15*). Such ox-

idation is also found with metals on amorphous supports. For Rh/Al_2O_3 van 't Blik *et al.* (*16*) report that Rh^+ gem–dicarbonyl clusters are formed on samples in which the Rh had originally been reduced to Rh^0; Basu *et al.* (*17*) suggest that this oxidative dispersion of rhodium is due to an interaction with isolated hydroxyl groups, i.e., oxidation by protons and release of hydrogen. Likewise, Juszczyk *et al.* (*18*) showed by FTIR of adsorbed CO on Pd/Al_2O_3 that Pd carrying a positive charge is formed by reaction with hydroxyl groups.

2. *Formation of Adducts of Metal Particles and Protons*

In view of the high metal–hydrogen bond strength, it is conceivable that protons react with metal particles, resulting in a positively charged metal particle with one or more adsorbed hydrogen atoms, e.g.,

$$Pd_n + zH^+ \rightarrow [Pdn\text{-}H_z]^{z+}. \qquad (4)$$

In other words, not all hydrogen atoms that are consumed in metal reduction will end up as protons bonded to oxygen ions of a cage wall, but some of these hydrogen atoms remain bonded to palladium atoms. In this hypothetical species, the positive charge will be distributed over the palladium and hydrogen atoms; the particle will thus be "electron-deficient." That could lead to enhanced catalytic activity, as Dalla Betta and Boudart have shown that electron-deficient Pt in Y-type zeolites containing multivalent cations is 40 times more active than Pt on amorphous supports toward hydrogenolysis of neopentane (*19*). Juszczyk *et al.* observed a catalytic superactivity for neopentane formation for Pd/Al_2O_3 after partial oxidation of the Pd particles (*18*). Gallezot *et al.* found that the extent of electron deficiency of zeolite-supported metals increases with the acidity of the zeolite (*20*). Tri *et al.* concur, finding a correlation between the electrophilic character of Pt as measured from X-ray absorption edge spectroscopy and the rate of hydrogenolysis of *n*-butane (*21*). Formation of a positively charged adduct with zeolite protons has recently been suggested by Sheu *et al.* for zeolite-encaged Pd carbonyl clusters on the basis of FTIR data of both the carbonyl ligands and the zeolitic O–H groups (*22*).

The interaction of protons with the very small metal particles in zeolite cages might differ from that with larger metal particles. Baetzold used extended Hückel and CNDO procedures for computing the electronic properties of Pd clusters (*23, 24*). He concludes that Pd aggregates up to 10 atoms have different electronic properties than larger particles because diffuse *s* atomic orbitals overlap strongly and form low-energy symmetric orbitals. As a consequence, vacant *d*-holes are created; the electron affinity for a Pd_{10} cluster is calculated to be 8.1 eV, well above the value of the electronic work function of bulk Pd (4.5 eV). Pd clusters of this size are more likely to be stabilized in zeolite cages than on the surface of amorphous supports. Indeed, the recent discovery of dramatically different FTIR spectra of CO adsorbed on Pd_n particles in Pd/NaY illustrates that the chemical properties of very small, zeolite-encaged Pd_n particles differ markedly from those of bulk Pd (*25*).

3. *Carbenium Ion Reactions of Hydrocarbons*

Zeolite protons are known to be strong Brønsted acid sites, rendering metal/zeolite catalysts bifunctional. In previous work by Chow *et al.* (*8*), it was shown that ring enlargement of methylcyclopentane is a sensitive probe for the catalytic function of zeolite protons. When their concentration is negligible, the sole reaction detectable with methylcyclopentane/hydrogen mixtures is ring opening, a reaction specific for the metal function (*26*). Moretti *et al.* (*6*) showed for PtCu/NaY that the ring enlargement selectivity of the reduced catalyst increased due to the protons created during metal reduction.

4. Formation of Carbonaceous Overlayers

Hydrocarbon conversion catalysis is generally accompanied by formation of carbonaceous residues, both on the metal particles and on the acid sites of bifunctional catalysts. Both types of "coke" have been identified by typical peaks in temperature-programmed oxidation (vide infra). On the acid sites, coke is formed by interaction, e.g., of olefins and carbenium ions. The olefins are companions of paraffins or cycloparaffins when these are in contact with reduced transition metals at a temperature where dehydrogenation reactions are catalyzed. Parera *et al.* studied the extent of coking on Pt/Al_2O_3 catalysts using a naphtha feed doped with various hydrocarbons (*27*). Their results show that the highest coke depositions occurred when the feed was doped with cyclopentane, cyclopentene, or cyclopentadiene. The metal particles are partially covered with coke in the early stages of the catalytic process; coke on the acid sites increases with extended times on stream. Barbier *et al.* have presented a mechanism for coke formation from C-5 rings over bifunctional catalysts involving olefin formation on a metal site followed by an acid-catalyzed condensation reaction (*28*). Although a different mechanism will govern coke formation on metal sites, it can be anticipated that the total amount of coke which is deposited on the catalyst during conversion of methylcyclopentane is likely to increase with the acidity of bifunctional metal/zeolite catalysts.

On the other hand, neopentane, 2,2 dimethylpropane (22DMP), which is unable to form olefins or secondary or tertiary carbenium ions, could leave bifunctional catalysts in its virgin form; i.e., deactivation has been reported to be negligible, even for catalysts exhibiting strong acid sites. This is one of the reasons why neopentane has often been used in fundamental work on catalysis. The absence of any acid-catalyzed conversion of neopentane under the conditions used in this paper was verified by replacing Pd/NaY by transition metal-free HY of high acidity. We should mention, however, that the primary products of this metal-catalyzed conversion will undergo secondary reactions including those catalyzed by acid sites. Therefore, the reaction rate of neopentane conversion is specific for the catalytic activity of the metal, but the product distribution reflects the action of both types of sites in bifunctional catalysis. In this paper we focus on the reaction rate; the product distribution has been described in detail in Ref. (*4*). It was for this reaction that Juszczyk *et al.* (*29*) reported with Pd/Al_2O_3 a turnover frequency (TOF) two orders of magnitude higher than that with Pd/SiO_2 and a further increase after treatments which resulted in partially oxidized particles (*18*).

Summing up, the above considerations motivate research described in this paper. The underlying working hypothesis, in its simplest form, might be formulated as follows: Neopentane conversion over reduced Pd/NaY should reveal an enhanced catalytic activity due to formation of electron deficient $[Pdn\text{-}H_z]^{z+}$ clusters, if such a superactivity really exists. If so, the enhanced activity (in comparison to that of Pd/SiO_2) should increase with the concentration of the protons. Methylcyclopentane conversion over the same catalysts should show how the enhanced activity of the metal, as revealed with neopentane, is superimposed by catalyst deactivation. The coke deposit will be characterized by temperature-programmed oxidation of the used catalysts.

II. EXPERIMENTAL

1. Sample Preparation and Pretreatment

Three Pd/NaY catalysts were prepared: Pd/NaY with Pd loadings of 2, 4, and 7 wt%. The catalysts were prepared by ion exchange of a dilute solution (0.1 *M*) of $Pd(NH_3)_4(NO_3)_2$ (Strem Chemicals, Lot 121640-S) with a NaY slurry (200 ml/g zeolite). The zeolite used was Linde LZ-52

whose approximate unit cell formula is $Na_{56}(AlO_2)_{56}(SiO_2)_{136}$. The exchange was performed according to the procedure described elsewhere (*9*). After drying in air at room temperature (RT), the palladium loadings were verified by chemical analysis performed by Galbraith Laboratories. Before kinetic runs the catalysts were calcined and reduced *in situ*. The pretreatment conditions were selected on the basis of our previous experience (*9–11*).

After ion exchange, two types of pretreatment conditions were used on the Pd/NaY samples, resulting in two groups of catalysts: series Pd/NaY-250 and series Pd/NaY-500. For both series calcination was performed in an O_2 flow (UHP, Matheson, U.S.A.; 180 ml/min), while the temperature was ramped at 0.5°C/min to either 250 or 500°C, and then held at the respective temperature for 2 hr. The oxygen was purified by passing over Pt/SiO_2 and the 4-Å molecular sieve cooled by dry ice. After calcination the samples were cooled to RT in helium (UHP, Matheson, U.S.A.; 30 ml/min) and reduced in H_2 (UHP, Matheson, U.S.A.; 25 ml/min). For the Pd/NaY-250 series, the reduction was followed from RT to 300°C, whereas, in the case of Pd/NaY-500 series, the reduction temperature was increased up to 350°C. In both cases, the same temperature program, dT/dt = 8°C/min, was applied. Metal dispersions (CO/Pd) of Pd/NaY catalysts pretreated as above follow from our previous work (*4*). Turnover frequencies are then expressed in terms of Pd surface atoms which are accessible to reaction with MCP or 22DMP.

An attempt to neutralize the protons formed during reduction of the Pd ions in the Pd/NaY-500 series was made. The reduced catalysts were then reslurried in doubly distilled water (200 ml/g catalyst). The pH of the resultant slurry was adjusted to pH 7–8 by slow, dropwise addition of dilute NaOH. The samples were then filtered, washed, and dried at RT in air. Prior to reaction, the samples were dehydrated in a He flow at 300°C for 2 hr, oxidized at 300°C for 1 hr, and reduced at 300°C for 1 hr.

The Pd/SiO_2 samples were prepared by a conventional impregnation technique; details on their preparation and characterization are described elsewhere (*30*).

2. Neopentane Conversion

The reactions of neopentane (= 2,2-dimethylpropane, further abbreviated as 22DMP) with hydrogen over the Pd/NaY samples and a Pd/SiO_2 sample were carried out in a fully automated continuous flow fixed bed reactor described in detail elsewhere (*4*). Turnover frequencies were calculated on the basis of accessible Pd surface atom as measured by CO chemisorption (*4*). Due to the differences in activity for series 250 and series 500, it was necessary to select proper ranges for the reaction temperature, T_{RXN} (for Pd/NaY-250, T_{RXN} = 240–280°C; for Pd/NaY-500, T_{RXN} = 210–250°C; and for Pd/SiO_2, T_{RXN} = 250–300°C). In all cases the conversion levels were kept below 10% and the reaction temperatures were always below the reduction temperatures ensuring that deactivation due to metal sintering was negligible.

3. Methylcyclopentane Conversion

As mentioned above, the catalysts were calcined and reduced with hydrogen, which was purified by passing over MnO/SiO_2 at RT and then through a 4-Å molecular sieve which was cooled by dry ice. The samples were then cooled under a H_2 flow to the reaction temperature. The MCP reaction was carried out on approximately 150 mg of the appropriate catalyst in a continuous flow microreactor under atmospheric pressure (*8*), 275°C, with a H_2/MCP ratio of about 18. The reaction mixtures were obtained by passing the purified H_2 through a MCP saturator cooled to 0°C by an ice/water bath. The MCP was purchased from Baker and was further purified using a 5-Å molecular sieve. The reaction flow rates were held constant at 20 ml/min and the

amount of catalyst used was adjusted in order to stay below 15% conversion. Reaction products were analyzed by an on-line HP 5794 gas chromatograph with a 50-m crosslinked methylsilicone fused capillary column equipped with a FID detector.

4. Temperature-Programmed Oxidation (TPO)

Temperature programmed oxidation was performed on selected catalysts after 22DMP and MCP reactions in a system described elsewhere (*31*). This instrument utilizes an on-line mass spectrometer as a detector, allowing for simultaneous *in situ* analysis of oxygen consumption and product formation. After reaction to the specified times, the catalysts were cooled in flowing He (60 ml/min), sealed, and transferred to the TPO system. After evacuation and repeated purging in Ar, the samples were cooled to −80°C in an Ar flow. TPO was performed in a 5% O_2/He flow (60 ml/min) with a temperature ramp of 8°C/min from −80°C to 550°C. Oxidation products were monitored using an on-line Dycor M200 mass spectrometer downstream from the reactor. In all cases the rate of O_2 consumption mirrors the rate of CO_2 evolution; only the CO_2 profiles are shown in an effort to save space. The carbon-to-accessible surface Pd (C/Pd) ratios were calculated assuming complete oxidation of the coke to CO_2. This assumption was confirmed by monitoring the CO signal, which was found to be of the order predicted by the Boudouard equilibrium.

III. RESULTS

1. Neopentane Conversion

Reaction rates and product distributions for the catalysts under study have been reported previously (*4*). The catalysts display remarkable stability; virtually no deactivation is observed during determination of the Arrhenius plots; i.e., the same selectivities and rates are observed when returning to the initial reaction temperature at the end of the run. As an example, Fig. 1 shows the data points used to describe the Arrhenius line for a 2-wt% Pd/NaY-250 catalyst. As shown in our previous paper, the high reproducibility of the kinetic data evidenced extends to all catalysts studied (*4*). This justifies the presentation of simple straight Arrhenius lines in the present paper for all catalysts studied in Fig. 2. From this it is

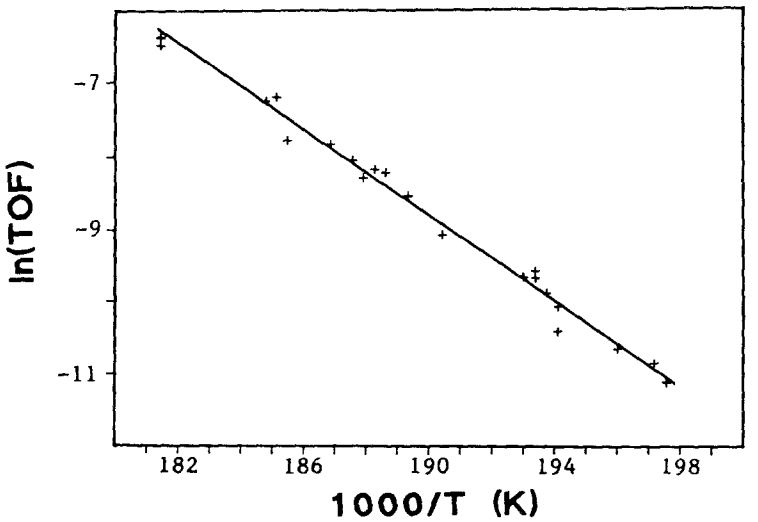

FIG. 1. Turnover frequencies (TOF) of neopentane conversion over 2 wt% Pd/NaY-250 catalyst displayed as an Arrhenius plot (ln(TOF) vs 1/T).

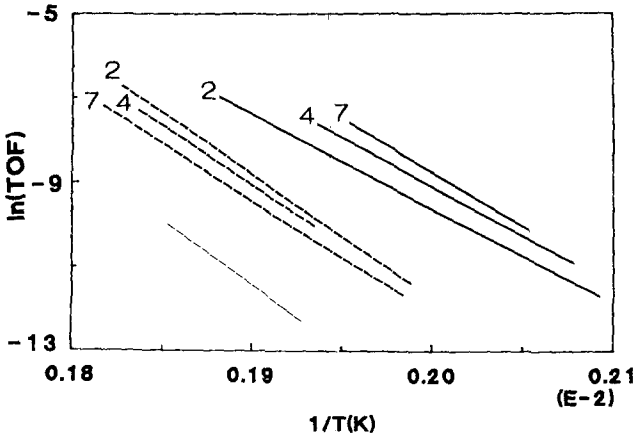

FIG. 2. Arrhenius plots for neopentane conversion over: (—) 2, 4, and 7 wt% Pd/NaY-500; (---) 2, 4, and 7 wt% Pd/NaY-250; (–––) 0.7 wt% Pd/SiO_2.

obvious that the catalytic activity of the catalysts considered follows the trend: Pd/NaY-500 series > Pd/NaY series > Pd/SiO_2.

In a previous paper we showed that, for a Pd particle which fills a supercage, approximately half of the surface atoms of a Pd particle inside a supercage are exposed to molecules through the supercage apertures and are therefore active for hydrocarbon conversion (*4*). For such particles chemisorption of CO gives a more realistic impression of the number of accessible metal sites than chemisorption of hydrogen, since adsorbed H atoms can easily migrate to those Pd atoms of an encaged particle which do not face cage windows. Therefore, all turnover frequency data in the present paper are expressed in the units: 10^{-4} molecules converted per second per accessible surface Pd as detected by CO adsorption.

2. *Methylcyclopentane Conversion*

Conversions and product distributions are presented in Table 1 for 5 and 95 min time on stream (TOS). It can be seen that, for the Pd/NaY-250 and Pd/NaY-500 series, ring-opening hydrogenolysis is initially the dominant reaction, but ring enlargement predominates at long TOS. The turnover frequency and the selectivities toward hydrogenolysis and ring enlargement are plotted versus TOS in Fig. 3. The data presented in Table 1 show that neutralization of the acidic sites by NaOH treatment sup-

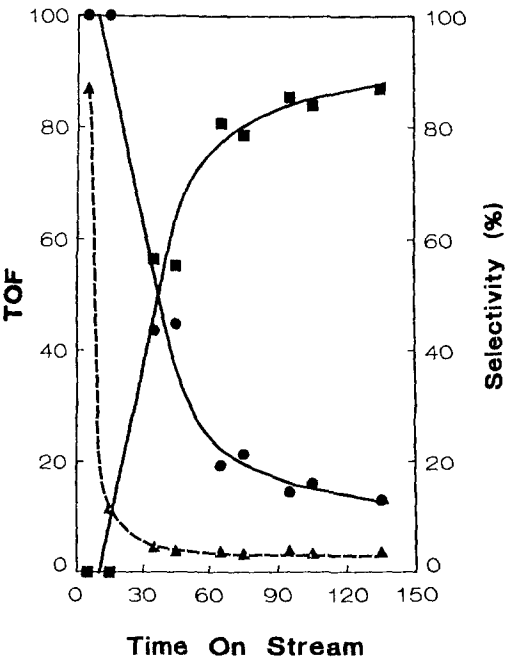

FIG. 3. TOF (▲) and selectivity toward hydrogenolysis (●) and ring enlargement (■) in the MCP reaction over a 7-wt% Pd/NaY-250 catalyst vs TOS.

TABLE 1

Conversion and Product Distribution of MCP Reaction

	Catalyst							
	Pd/NaY-250			Pd/NaY-500			Neutralized Pd/NaY-500	Pd/SiO_2
	7 wt%	4 wt%	2 wt%	7 wt%	4 wt%	2 wt%	2 wt%	0.76 wt%
	5 Min time on stream							
Total conversion (%)	13.4	11.4	7.4	6.4	6.5	6.0	12.5	14.5
Product Distribution[a]								
Methane	2.6	2.4	2.1	2.0	2.4	1.7	0.9	—
Ethane	—	—	—	—	—	—	—	—
Propane	—	—	—	—	—	—	—	—
i-Butane	—	—	—	—	—	—	—	—
n-Butane	—	—	—	—	—	—	—	—
i-Pentane	1.1	0.9	0.7	1.8	1.5	1.3	0.7	—
n-Pentane	0.7	—	—	3.8	2.5	1.9	0.7	—
Cyclopentane	9.9	9.1	8.3	1.7	5.5	5.3	3.7	1.0
2,2-Dimethylbutane	—	—	—	—	—	—	—	—
2,3-Dimethylbutane	—	—	—	—	—	—	—	—
2-Methylpentane	45.0	46.2	47.1	42.5	44.9	46.1	48.9	46.0
3-Methylpentane	25.4	26.1	26.4	27.2	26.8	26.9	26.3	26.5
n-Hexane	15.5	15.3	15.4	17.5	16.8	16.9	18.8	26.5
Benzene	—	—	—	1.7	—	—	—	—
Cyclohexane	—	—	—	1.8	—	—	—	—
	95 Min time on stream							
Total conversion (%)	0.6	0.6	0.7	1.4	0.7	0.6	0.9	4.0
Product Distribution[a]								
Methane	—	—	—	—	—	—	—	—
Ethane	—	—	—	—	—	—	—	—
Propane	—	—	—	—	—	—	—	—
i-Butane	—	—	—	—	—	—	—	—
n-Butane	—	—	—	—	—	—	—	—
i-Pentane	—	—	—	—	—	—	—	—
n-Pentane	—	—	—	—	—	—	—	—
Cyclopentane	—	—	—	—	—	—	—	1.2
2,2-Dimethylbutane	—	—	—	—	—	—	—	—
2,3-Dimethylbutane	—	—	—	—	—	—	—	—
2-Methylpentane	12.6	17.7	40.5	—	—	12.0	56.5	47.1
3-Methylpentane	—	—	21.5	—	—	—	27.5	26.2
n-Hexane	1.9	5.7	11.2	—	—	4.1	16.0	25.5
Benzene	42.3	40.5	10.3	42.0	39.0	37.0	—	—
Cyclohexane	43.1	36.1	16.5	58.0	61.0	47.0	—	—

[a] Moles per 100 moles methylcyclopentane converted.

presses formation of cyclohexane and benzene, resulting in catalytic behavior similar to Pd/SiO_2. This is in agreement with previous results of Chow *et al.* (*8*) that, for Pt/NaHY catalysts and at the temperatures used here, ring opening hydrogenolysis is predominantly a metal-catalyzed reaction, but ring enlargement requires support acidity. A summary of the MCP selectivity data, including the 2-methylpentane/3-

TABLE 2

Methylcyclopentane Conversion on Pd Catalysts with Different Support Acidities

	TOF[a]		Selectivity (%) DH[c]		RO[d]		RE[e]		2MP/3MP 5	3MP/*n*HEX 5
TOS[b]	5	95	5	95	5	95	5	95		
Catalyst										
Pd/NaY-500										
7 wt%	14.1	3.2	9.3	—	87.2	—	3.5	100.0	1.6	1.6
4 wt%	21.9	2.5	11.9	—	88.1	—	—	100.0	1.7	1.6
2 wt%	22.3	2.1	10.1	—	89.9	16.1	—	83.9	1.7	1.6
Pd/NaY-250										
7 wt%	86.9	4.0	14.2	—	85.8	14.6	—	85.4	1.8	1.6
4 wt%	50.0	2.8	12.5	—	87.6	23.5	—	76.6	1.8	1.7
2 wt%	39.0	3.8	11.1	—	90.0	73.2	—	26.8	1.8	1.7
Neutralized Pd/NaY-500										
2 wt%	52.5	3.7	6.0	—	94.0	100.0	—	—	1.9	1.4
Pd/SiO_2										
0.76 wt%	171.8	47.2	1.0	1.2	99.0	98.9	—	—	1.7	1.0

[a] (10^{-4} molecules MCP) (accessible Pd surface atom)$^{-1}$(sec)$^{-1}$.
[b] Time on stream (min).
[c] Deep hydrogenolysis.
[d] Ring opening.
[e] Ring enlargement.

methylpentane (2MP/3MP) and 3-methylpentane/*n*-hexane (3MP/nHEX) ratios, combined with the TOFs is presented in Table 2.

3. *Temperature-Programmed Oxidation*

In view of the detection limits of the mass spectrometer, TPO was performed on the higher Pd loading samples (7 wt%) after reaction of either 22DMP or MCP. As expected, no significant amount of coke was detected in the case of the 22DMP reaction, but coke formation was large after MCP reaction. The TPO profiles obtained after 125 min TOS in the MCP reaction are presented in Fig. 4 and the quantitative data are given in Table 3. The TPO profiles show two peaks ($T_{MAX} \approx 200$°C and $T_{MAX} \approx 350$°C).

IV. DISCUSSION

First, we shall compare the results of neopentane conversion over the catalysts studied and discuss them in terms of our current knowledge about the catalytic behavior of palladium in this reaction and re-

TABLE 3

Carbon Retention during Methylcyclopentane Conversion

Catalyst	C/Pd[a]
7 wt% Pd/NaY-500 after 125 min	11.2
7 wt% Pd/NaY-250 after 125 min	5.1
Neutralized 7 wt% Pd/NaY-500 after 125 min	1.3
1.5 wt% Pd/SiO_2 after 125 min	0.7

[a] Carbon per accessible Pd surface atom.

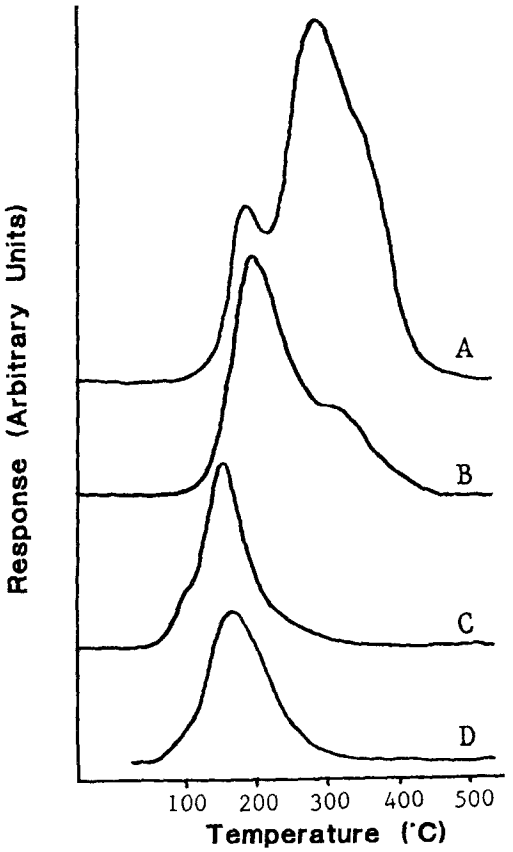

FIG. 4. CO_2 profiles obtained during TPO of catalysts after 125 min TOS of the MCP reaction. (A) 7 wt% Pd/NaY-500; (B) 7 wt% Pd/NaY-250; (C) neutralized 7 wt% Pd/NaY-500; (D) 1.45 wt% Pd/SiO_2.

cent FTIR results of CO adsorbed on these catalysts. We shall then propose a model for the active sites in Pd/NaY catalysts. Interpretation of the MCP reaction results will be based on this model in combination with the TPO data.

The product distributions for the neopentane reaction with H_2 over Pd/NaY (*4*) and Pd/SiO_2 (*30*) have been described in detail in earlier papers. Small changes in selectivity do not appear specific for the catalysts used in this study and, therefore, will not be discussed here. Instead, we wish to focus on the rather pronounced variations of the overall activity. The most striking result seen in Fig. 2 is that all Pd/NaY catalysts are much more active than Pd/SiO_2. More specifically, catalysts of the series Pd/NaY-250 are approximately 12 times more active than Pd/SiO_2 and those of series Pd/NaY-500 are about 150 times more active. The TOFs for the Pd/NaY-500 series catalysts extrapolated to $T_{RXN} \approx 260°C$ are well above 10^{-3} sec^{-1}, resembling the transient catalytic superactivity reported for certain alumina-supported Pd catalysts (*18*). For these, we had previously presented data from which it was concluded that Pd^{n+} ions, stabilized in vacant surface octahedral sites, are the sites responsible for the high catalytic activity for neopentane hydrogenolysis. The intensity of the IR bands characteristic of CO adsorbed on Pd^{n+} ions appeared to be well correlated to the catalytic activity. Pd^{n+} ions have also been shown, by Driessen *et al.*, to be part of the active sites catalyzing CO hydrogenation to methanol (*32*). Vannice attributes the enhanced methanation activity of Pd/HY compared to Pd/SiO_2 to the formation of weakly bound CO species on electron-deficient Pd particles (*33*). It is, therefore, tempting to relate the superior activity of our Pd/Y catalysts in neopentane conversion to "electron-deficient" Pd particles, as was done before by Dalla Betta and Boudart (*19*) for Pt/NaY and the same probe reaction.

Electron deficiency of metal particles on alumina has been ascribed to metal interaction with Lewis acid sites, which act as electron acceptors. For Pd particles supported in NaY, this seems less likely; it is possible, however, that electron-deficient Pd particles are actually $[Pd_n\text{-}H_z]^{z+}$ adducts. Their charge will, of course, not be localized on the hydrogen atoms, but smeared out over the particle. This model is supported by recent FTIR studies of CO adsorption on Pd/NaY samples, similar to those used in this study (*25*). The highly structured spectra show bands which are attributed to Pd carbonyl clusters occluded in the supercages; they include additional bands attributed to linear-bonded CO adsorbed on Pd^+ and $Pd^{\delta+}$. The FTIR data also indicate that zeolite protons interact

with these species, resulting in the formation of positively charged particles (*22*). We therefore suggest that these "electron-deficient" particles are potential candidates for the highly active sites in Pd/NaY catalyzing 22DMP conversion.

This model is strongly supported by the finding that the calcination temperature of the samples has a strong effect on their activity. Although differences in dispersion have already been eliminated by expressing the activities in terms of turnover frequencies (per *exposed* Pd surface atom), the sequence clearly is

$$\text{Pd/NaY-500} > \text{Pd/NaY-250} > \text{Pd/SiO}_2.$$

In the Introduction it was pointed out that, after reduction, the Pd/NaY-500 series contains a proton concentration equal to twice the number of Pd atoms; however, in the Pd/NaY-250 series, most of the protons are trapped as NH_4^+ ions. The activity sequence clearly follows the sequence in proton concentration, supporting the model of $[Pd_x\text{-}Hz]^{z+}$ adducts as sites of enhanced activity.

In a previous paper, a possible reaction pathway for Pd-catalyzed neopentane hydrogenolysis and isomerization was discussed, involving an $\alpha\gamma$ diadsorbed metallacyclobutane intermediate (*4*). This reaction path is entirely consistent with the present model. The concept that positively charged or "electron-deficient" Pd is responsible for the enhanced catalysis is also in agreement with results of a recent study by Tolbert *et al.* of the activation of alkanes by Pd^+ ions in the gas phase (*34*). In this study, it is concluded that interaction of Pd^+ with neopentane leads to insertion of Pd^+ into a C–C bond, followed by stripping off of CH_4.

Turning now to the MCP reaction, Table 2 shows that the trend in observed activity is reversed,

$$\text{Pd/SiO}_2 > \text{Pd/NaY-250} > \text{Pd/NaY-500},$$

and the amount of coke deposited for equal TOS (Table 3), as determined from integration of the CO_2 TPO profiles, follows the trend

$$\text{Pd/NaY-500} > \text{Pd/NaY-250} > \text{Pd/SiO}_2.$$

This trend matches that of the relative support acidities. Excessive coke formation is, therefore, ascribed to the presence of Brønsted sites, which initiate carbenium ion formation and condensation for the MCP reaction, but not for the 22DMP reaction.

Coke, as deposited on bifunctional catalysts under reforming conditions, is usually classified in two main categories: (a) coke on the metal (this species is known to give rise to a TPO peak maximum below 300°C), and (b) coke on acid sites (its TPO profile peaks above 300°C) (see Refs. *31*, *35–37*). Our data, presented in Fig. 4, agree with this: only the low-temperature peak is present in the case of Pd/SiO_2 which does not exhibit acid sites, but both peaks are present in the Pd/NaY-250 and especially the Pd/NaY-500 catalysts. It is also relevant that the size of the high-temperature TPO peak increases with increasing support acidity. Table 3 shows that the three Pd/NaY samples mainly differ in the quantity of this coke, which is virtually absent in Pd/SiO_2 and in the Pd/NaY sample, which had been treated with NaOH to neutralize acid sites. The deactivation of the Pd/NaY catalysts for MCP ring opening, however, reflects self-poisoning of metal sites. Therefore, the rate of initial deactivation, shown in Fig. 3 for Pd/NaY, is similar to that found for Pd/SiO_2. These samples, however, differ vastly in the amounts of coke accumulation. The steep decrease in MCP conversion rate after very brief TOS shows that the Pd ensembles required for this process are rapidly deactivated. Presumably, the Pd particles retain their activity for the much less structure-sensitive process of MCP dehydrogenation, so that the process of coke deposition on acid sites, via olefins and carbenium ions, continues for long TOS. This is confirmed by our TPO data, taken after various times on stream (not

shown): the low-temperature TPO peak shows almost full intensity after short TOS, whereas the high-temperature TPO peak continues to increase with TOS. Very similar evidence has been reported by Parera *et al.* (*38*) for industrial reforming catalysis; coke deposition on the metal particles slows down after an initial stage, but deposition on the acid sites continues with TOS. We noted above that the same catalysts are not deactivated under the conditions of 22DMP conversion; this evidence and the absence of any TPO peak show that with 22DMP no carbonaceous overlayer is formed on the metal particles.

Additional conclusions can be drawn from a comparison of the selectivities, both for different samples and for different times on stream. Two types of selectivities are of interest: (1) Ring opening/ring enlargement and relative ring opening rate of the three types of C–C bonds in the cyclopentane ring. In general, the change of selectivity with time on stream is similar to that found previously for Pt/NaY (*8*) and PtCu/NaY (*6*). Initially, the metal-catalyzed ring opening reaction prevails, but after partial deactivation of the metal function the ring enlargement tends to dominate the scene, as this acid-catalyzed reaction has a higher energy of activation. The primary product of ring enlargement is rapidly dehydrogenated even on partially deactivated metal particles, because dehydrogenation has the lowest ensemble requirement of all metal-catalyzed conversion of hydrocarbons.

The conversion and product distributions at 5 min TOS are shown in Tables 1 and 2 for both the Pd/NaY-250 series and the Pd/NaY-500 series. The data show that at low TOS, metal-catalyzed hydrogenolysis is the dominant reaction. This is in agreement with the product distributions for Pd/SiO_2, which has no acidic sites. Kranich *et al.* have shown NaOH neutralization of the protons to be effective for Pd supported in various zeolites (*39*). Our MCP results agree with this. The selectivity data show that the neutralized catalyst is incapable of forming ring enlargement products, which are indicative of acidic sites.

At long times (95 min TOS), metal-catalyzed hydrogenolysis declines and ring enlargement, which requires both metal and acidic sites, predominates. This behavior is illustrated in Fig. 3. Two causes will contribute to this pronounced change in selectivity with time on stream. First, a decrease in selectivity to hydrogenolysis with decreasing activity is expected as hydrogenolysis is an ensemble-sensitive reaction (*40*) and the number of suitable ensembles rapidly decreases due to site blocking by coke. In conformity with this, recent MCP work on PtCu/NaY catalyst showed that the addition of Cu, which breaks up the Pt ensembles, results in a marked decrease in hydrogenolysis yield (*6*). Ring enlargement, however, occurs through a bifunctional pathway (olefin formation on a metal site, followed by carbenium ion formation and subsequent ring enlargement on the acidic site); we noted already that the less ensemble-sensitive reaction of (de-)hydrogenation survives extensive deactivation of larger metal ensembles.

A second cause for the change in selectivity with time on stream is especially valid for the Pd/NaY-250 sample. The NH_4^+ ions which are present in this catalyst after reduction of the $Pd(NH_3)^{2+}$ ions might slowly decompose during MCP conversion, creating additional protons. Indeed, the C_6 ring products, which for this catalyst are totally absent at 5 min TOS, form a substantial fraction of the reaction product after 95 min TOS.

The selectivities with respect to the three possible ring-opening products are of interest. Assuming that all five C–C bonds have an equal probability for bond breaking, the statistical ring opening product distribution would be 2-methylpentane (2MP) : *n*-hexane (*n*-HEX) : 3-methylpentane (3MP) = 2 : 2 : 1. The ring-opening selectivities of our Pd/NaY samples differ from this value, but are the same for both the Pd/NaY-250 and the Pd/NaY-500 (Table 2). The approxi-

mate MCP ring-opening product ratios for our Pd/NaY catalysts are then 2MP:*n*-HEX:3MP = 1.8:0.6:1 and 2MP:*n*-HEX:3MP = 1.7:1:1 for Pd/SiO_2. It is obvious that the formation of *n*-HEX is suppressed when Pd is supported in the zeolite. This behavior has been found previously for Pt/NaY catalysts, and has been attributed to a steric hindrance of MCP rollover on the Pt particle by the zeolite lattice (*5, 41*). It is possible that the high 3MP/*n*-HEX ratios found for Pd/NaY are due to the same phenomenon.

V. CONCLUSIONS

Differences in the catalytic activity trends for the 22DMP reaction (Pd/NaY-500 > Pd/NaY-250 > Pd/SiO_2) and for the MCP reaction (Pd/SiO_2 > Pd/NaY-250 > Pd/NaY-500) can be correlated with the different concentration of zeolithic protons. Some protons appear to interact with reduced Pd particles forming "electron-deficient" $[Pd_n\text{-}H_z]^{z+}$ species, which are highly active in the conversion of neopentane. No catalyst deactivation and no coke formation is observed after 22DMP conversion. The MCP reaction induces "coke" formation on the metal particles; in addition the occurrence of carbenium ions leads to large amounts of coke on the acid sites, characterized by a TPO peak above 300°C. This type of coke is absent in Pd/SiO_2 and neutralized Pd/NaY. The deactivation of the Pd particles in Pd/NaY for metal-catalyzed MCP ring opening is rapid, in accordance with the high ensemble sensitivity of this process. Selective deactivation of the metal function in bifunctional catalysts changes the selectivity in favor of acid (co-)catalyzed ring enlargement. Neutralization of acid sites by NaOH renders the selectivities and the coke formation characteristics of Pd/NaY similar to those of Pd/SiO_2.

ACKNOWLEDGMENTS

Support from the U.S. Department of Energy under Contract DE-FG02-87ERA3654 and grants in aid from the Engelhard Co. and the EXXON Education Foundation are gratefully acknowledged.

REFERENCES

1. Gallezot, P., and Bergeret, G., *in* "Catalyst Deactivation" (E. E. Peterson and A. T. Bell, Eds.), p. 263. Dekker, New York (1987).
2. Sachtler, W. M. H., Tzou, M. S., and Jiang, H. I., *Solid State Ionics* **26,** 71 (1988).
3. Homeyer, S. T., and Sachtler, W. M. H., *in* "Zeolites: Facts, Figures, Future" (P. A. Jacobs, and R. A. van Santen, Eds.), p. 975. Elsevier, Amsterdam (1989).
4. Homeyer, S. T., Karpiński, Z., and Sachtler, W. M. H., *Recl. Trav. Chim. Pays-Bas* **109,** 81 (1990).
5. Jiang, H. J., Tzou, M. S., and Sachtler, W. M. H., *Appl. Catal.* **39,** 255 (1988).
6. Moretti, G., and Sachtler, W. M. H., *J. Catal.* **115,** 205 (1989).
7. Moretti, G., and Sachtler, W. M. H., *J. Catal.* **116,** 350 (1989).
8. Chow, M., Park, S. H., and Sachtler, W. M. H., *Appl. Catal.* **19,** 349 (1985).
9. Homeyer, S. T., and Sachtler, W. M. H., *J. Catal.* **117,** 91 (1989).
10. Homeyer, S. T., and Sachtler, W. M. H., *J. Catal.* **118,** 266 (1989).
11. Homeyer, S. T., and Sachtler, W. M. H., *Appl. Catal.* **54,** 189 (1989).
12. Dessau, R. M., *J. Catal.* **77,** 304 (1982).
13. Tzou, M. S., and Sachtler, W. M. H., *in* "Catalysis 1987" (J. W. Ward, Ed.), p. 233. Elsevier, Amsterdam (1988).
14. Tzou, M. S., Teo, B. K., and Sachtler, W. M. H., *J. Catal.* **113,** 220 (1988).
15. Tzou, M. S., Jiang, H. J., and Sachtler, W. M. H., *Reac. Kinet. Catal. Lett.* **35,** 207 (1987).
16. van 't Blik, H. F. J., van Zon, J. B. A. D., Huizinga, T., Vis, J. C., Koningsberger, D. C., and Prins, R., *J. Amer. Chem. Soc.* **107,** 3139 (1985).
17. Basu, P., Panayotov, D., and Yates, J. T., *J. Phys. Chem.* **91,** 3133 (1987).
18. Juszczyk, W., Karpiński, Z., Ratajczykowa, I., Stanasiuk, Z., Zieliński, J., Sheu, L. L., and Sachtler, W. M. H., *J. Catal.* **120,** 68 (1989).
19. Dalla Betta, R. A., and Boudart, M., *in* "Proceedings, 5th International Congress on Catalysis, Palm Beach, 1972" (J. W. Hightower, Ed.), p. 1329. North-Holland, Amsterdam, 1973.
20. Gallezot, P., *Catal. Rev. Sci. Eng.* **20,** 121 (1979).
21. Tri, T. M., Massardier, J., Gallezot, P., and Imelik, B., *in* "Proceedings, 7th International Congress on Catalysis, Tokyo, 1980" (T. Seiyama and K. Tanabe, Eds.), p. 266. Elsevier, Amsterdam, 1981.
22. Sheu, L. L., Knözinger, H., and Sachtler, W. M. H., *J. Amer. Chem. Soc.* **111,** 8125 (1989).

23. Baetzold, R. C., *J. Chem. Phys.* **55,** 4363 (1971).
24. Baetzold, R. C., *J. Catal.* **29,** 129 (1973).
25. Sheu, L. L., Knözinger, and Sachtler, W. M. H., *Catal. Lett.* **2,** 129 (1989).
26. Gault, F. G., *in* "Advances in Catalysis" (D. D. Eley, H. Pines, and P. B. Weisz, Eds.), Vol. 30, p. 1. Academic Press, New York, 1981.
27. Parera, J. M., Figoli, J. N., Beltramini, E. J., Churin, E. J., and Cabrol, R. A., *in* "Proceedings, 8th International Congress on Catalysis, Berlin, 1984," Vol. 2, p. 593. Dechema, Frankfurt-am-Main, 1984.
28. Barbier, J., Elassal, L., Gnep, N. S., Guisnet, M., Molina, W., Zhang, Y. R., Bournonville, J. P., Frank, J. P., *Bull. Soc. Chem. France* **1,** 250 (1984).
29. Juszczyk, W., Karpiński, Z., Pielaszek, J., Ratajczykowa, I., and Stanasiuk, Z., *in* "Proceedings, 9th International Congress on Catalysis, Calgary, 1988" (M. J. Phillips and M. Ternan, Eds.), Vol. 3, p. 1238. Chem. Institute of Canada, Ottawa, 1988.
30. Karpiński, Z., Butt, J. B., and Sachtler, W. M. H., *J. Catal.* **119,** 521 (1989).
31. Augustine, S. M., Alameddin, G. N., and Sachtler, W. M. H., *J. Catal.* **115,** 217 (1989).
32. Driessen, J. M., Poels, E. K., Hindermann, J. P., and Ponec, V., *J. Catal.* **82,** 26 (1983).
33. Vannice, M. A., *J. Catal.* **40,** 129 (1975).
34. Tolbert, M. A., Mandich, M. L., Halle, L. F., and Beauchamp, J. L., *J. Amer. Chem. Soc.* **108,** 5675 (1986).
35. Biswas, J., Bickle, G. M., Gray, P. G., Do, D. D., and Barbier, J., *Catal. Rev. Sci Eng.* **30,** 161 (1988).
36. Barbier, J., *in* "Catalyst Deactivation 1987" (B. Delmon and G. F. Froment, Eds.), p. 1. Elsevier, Amsterdam (1987).
37. Parera, J. M., Figoli, J. N., Beltramini, E. J., Churin, E. J., and Cabrol, R. A., *in* "Proceedings, 8th International Congress on Catalysis, Berlin, 1984," Vol. 2, p. 593. Dechema, Frankfurt-am-Main, 1984.
38. Parera, J. M., Querini, C. A., and Figoli, N. S., *Appl. Catal.* **44,** L1–L8 (1988).
39. Kranich, W., Weiss, A., Schay, Z., and Guzi, L., *Appl. Catal.* **13,** 257 (1985).
40. Sachtler, W. M. H., and van Santen, R. A., *in* "Advances in Catalysis" (D. D. Eley, H. Pines, and P. B. Weisz, Eds.), Vol. 26, p. 69. Academic Press, New York, 1977.
41. Sachtler, W. M. H., *Ultramicroscopy* **20,** 135 (1986).